

Multiple effects of KPQ deletion mutation on gating of human cardiac Na⁺ channels expressed in mammalian cells

RASHMI CHANDRA, C. FRANK STARMER, AND AUGUSTUS O. GRANT
Duke University Medical Center, Durham, North Carolina 27710

Chandra, Rashmi, C. Frank Starmer, and Augustus O. Grant. Multiple effects of KPQ deletion mutation on gating of human cardiac Na⁺ channels expressed in mammalian cells. *Am. J. Physiol.* 274 (*Heart Circ. Physiol.* 43): H1643–H1654, 1998.—Several aspects of the effect of the KPQ deletion mutation on Na⁺ channel gating remain unresolved. We have analyzed the kinetics of the early and late currents by recording whole cell and single-channel currents in a human embryonic kidney (HEK) cell line (HEK293) expressing wild-type and KPQ deletion mutation in cardiac Na⁺ channels. The rate of inactivation increased three- to fivefold between –40 and –80 mV in the mutant channel. The rate of recovery from inactivation was increased twofold. Two modes of gating accounted for the late current: 1) isolated brief openings with open times that were weakly voltage dependent and the same as the initial transient and 2) bursts of opening with highly voltage-dependent prolonged open times. Latency to first opening was accelerated, suggesting an acceleration of the rate of activation. The ΔKPQ mutation has multiple effects on activation and inactivation. The aggregate effects may account for the increased susceptibility to arrhythmias.

long Q-T syndrome; sodium channel; embryonic kidney cells; patch clamp

RECENT STUDIES HAVE SHOWN that the genetic defect in a subgroup of patients with the autosomal dominant form of the long Q-T syndrome is linked to mutations in the cardiac Na⁺ channel α-subunit gene on the short arm of chromosome 3 (37, 38). The most severe defect is a deletion mutation of nine bases that code for Lys-1505, Pro-1506, Gln-1507 in the linker between domains III and IV of the Na⁺ channel α-subunit. Prior studies have shown that this linker is a highly conserved region of the Na⁺ channel and plays a central role in inactivation (15, 30, 36, 41).

Initial reports using heterologous expression of the mutant Na⁺ channel α-subunit in frog oocytes by Bennett et al. (6) and Dumaine et al. (10) demonstrated a small component of Na⁺ current that persisted after termination of the initial transient. This late component of Na⁺ current could prolong the duration of the cardiac action potential and the Q-T interval of the surface electrocardiogram (ECG). There is some controversy as to the nature of the persistent current and of the effect of the KPQ deletion mutation on other aspects of Na⁺ channel gating (6, 10). In their initial report, Bennett et al. reported an acceleration of the macroscopic inactivation of the current, whereas Dumaine et al. reported no change. Bennett et al. described a single mode of gating, with bursts accounting for the late current. Dumaine et al. suggested two modes of gating accounting for the late current: isolated openings and bursts of openings. Neither study pro-

vided data on the time dependence of late events. When the Na⁺ channel α-subunit of the brain and skeletal muscle is expressed in frog oocytes, the inactivation kinetics are slower than those of the native channel (20, 22). This change in gating is corrected by coexpression of the α- and β-subunits (18). In the case of the cardiac Na⁺ channel, the data are controversial, with studies showing no effect or an acceleration of inactivation with β-subunit coexpression (24, 26). The large size of the oocyte and the geometric complexity of its surface membrane limit its utility in the analysis of Na⁺ channel kinetics (21, 25). Bennett et al. reexamined the gating kinetics of the long Q-T interval-associated mutant channels expressed in a mammalian cell line using whole cell recordings. In contrast to their earlier studies in the frog oocytes, they showed an acceleration of recovery from inactivation. Their data also suggested that overlap in the activation and inactivation curves also contributes to the late current, a conclusion that differs from that of Dumaine et al. (10).

We have examined the kinetics of gating of the wild-type and ΔKPQ mutant Na⁺ channel α-subunit stably expressed in a human embryonic kidney (HEK) cell line (HEK293). The small size and spherical shape of the HEK293 cells permit rapid voltage clamping. The Na⁺ channel kinetics more closely resemble those in the native cells (33). We have combined whole cell and single-channel recordings to determine the basis of the persistent current and the other effects of the KPQ deletion on channel gating. By combining whole cell and single-channel recordings, it was possible to relate changes in the whole cell current waveform to the underlying changes in gating. Our results show that the KPQ deletion has a wide range of effects on both the activation and inactivation of the Na⁺ channel. Robust persistent currents were observed at potentials of –20 and –10 mV, well outside the range of activation and inactivation overlap but sufficiently depolarized to contribute to prolongation of the plateau of the action potential. The composite effects of the mutation on gating may be important in the increased susceptibility to arrhythmias in patients with this mutation.

METHODS

Construction of hH1 and deletion mutant KPQ/hH1. The 5' segment of the human cardiac Na⁺ channel gene hH1 from the starting Met at a position 150 bp to the *Xho*I site at 683 bp was synthesized using polymerase chain reaction (PCR). A *Hind* III site was introduced preceding the ATG codon to facilitate cloning of the 5' end. The PCR product was restricted with *Hind* III and *Xho* I and cloned into the corresponding sites in pREP4 plasmid (Invitrogen, San Diego, CA). hH1 in pSP64 parent plasmid (clone generously provided by Dr. A. George) was restricted with *Xho* I and *Sfi* I. The ~5.5-kb band was excised and cloned into the corresponding

sites in pREP4. The *Sfi* I site had to be repaired in both the plasmid and insert because the sequence of the site was different.

To perform the Δ KPQ mutation, hH1 was first cloned into pcDNA3 (Invitrogen) by using the above strategy, except the *Sfi* I repaired end of hH1 was ligated to the *Xba* I repaired end of pcDNA3. The deletion of KPQ was done by recombinant PCR (16). The PCR product carrying the mutation was restricted with *Kpn* I and *Bst*E II and used to replace the wild-type segment in hH1. All PCR products were sequenced in their entirety by using the chain termination method of Sanger et al. (32).

Expression of hH1 and KPQ deletion mutant in mammalian cells. DNA (10 μ g) was transfected into 293-EBNA cells (pREP4 plasmid) or HEK293 cells (pcDNA3 plasmid) by using Lipofectamine (GIBCO-BRL, Gaithersburg, MD) in DMEM without serum or antibiotics. After 4 h of incubation at 37°C, an equal amount of DMEM containing 20% FBS was added to the medium over transfected cells. After 24 h of transfection the cells were trypsinized, counted, and aliquoted into a 96-well plate at a density of 10,000 cells/well. Individual colonies were picked, grown, and tested for Na⁺ channel expression by whole cell voltage clamping.

Cells transfected with hH1 cloned in pREP4 were grown and selected in DMEM containing 10% FBS, nonessential amino acids, penicillin (100 U/ml), streptomycin (100 μ g/ml), and hygromycin (300–500 μ g/ml; Boehringer Mannheim, Indianapolis, IN). Cells transfected with KPQ deletion mutant cloned in pcDNA3 were grown and selected in DMEM containing 10% FBS, penicillin (100 U/ml), streptomycin (100 μ g/ml), and G-418 (500 μ g/ml; GIBCO-BRL).

Experimental setup. A coverslip containing cultured HEK293 cells was superfused in a tissue bath for at least 10 min before recordings were initiated. For whole cell recordings, cells were perfused with an Na⁺ external solution. Micropipettes were filled with a Cs⁺ internal solution. The internal Cs⁺ block the endogenous K⁺ current in these cells. The only ionic current measured under these conditions is Na⁺ current. For single-channel recordings, cells were perfused with a high-K⁺ solution. This solution reduced the membrane potential to 0 mV. Membrane potential is reported as absolute values. Na⁺ and K⁺ were the major cations in the microelectrode solution. Occasionally (<1% of trials), we observed long single-channel openings that apparently did not result from the opening of Na⁺ channels; the current was outward between –30 and 0 mV. Single Na⁺ channel currents were inward in this potential range. The outward channel openings are probably the endogenous K⁺ currents resolved at the single-channel level. Depolarizing trials showing outward currents were excluded from analysis.

The Na⁺ external solution used in the electrophysiology experiments had the following composition (in mM): 130 NaCl, 4 KCl, 1 CaCl₂, 5 MgCl₂, 5 HEPES, and 5 glucose; pH was adjusted to 7.4 with NaOH. The composition of the Cs⁺ micropipette solution was (in mM) 130 CsCl, 1 MgCl₂, 5 MgATP, 10 1,2-bis(2-aminophenoxy)ethane-*N,N,N,N'*-tetraacetic acid, and 10 HEPES; pH was adjusted to 7.2 with CsOH. High-K⁺ external solution consisted of (in mM) 140 K-aspartate, 10 KCl, 2 MgCl₂, 1 CaCl₂, 5 glucose, and 5 HEPES; pH was adjusted to 7.4 with KOH. The composition of the Na⁺ micropipette solution was (in mM) 140 NaCl, 5 KCl, 2.5 MgCl₂, 0.2 CaCl₂, and 5 HEPES; pH was adjusted to 7.4 with NaOH. All experiments were performed at room temperature (20–22°C).

Recording techniques. Whole cell and single-channel currents were recorded with an integrating patch-clamp amplifier (model 3900 A, Dagan, Minneapolis, MN) with a whole

cell expander module (model 3911 A, Dagan). Whole cell currents were recorded with 0.5- to 1.5-M Ω microelectrodes. An Ag-AgCl electrode wire coupled each microelectrode to the input of the amplifier. A similar wire embedded in agar-micropipette solution formed the bath reference. Series resistance compensation was achieved using conventional and supercharging techniques (4). Each whole cell voltage-clamp experiment started with an assessment of adequacy of voltage control, as previously described (11). The holding potential was set at –100 mV. Stable whole cell recordings could not be obtained in these cells for prolonged periods at hyperpolarized potentials. The current-voltage relationship was determined with 20-ms pulses of increasing amplitude applied at 1,000-ms intervals. The pulse amplitude was incremented in 5-mV steps from a potential of –60 to +60 mV. The steady-state inactivation curve was determined by the application of 200-ms prepulses from –130 to +55 mV. A 20-ms test pulse to –20 mV followed the prepulse. The prepulse potential was incremented in 5-mV steps. The development of inactivation was determined at –40, –60, and –80 mV by application of prepulses of increasing duration followed by a test pulse to –20 mV. Recovery from inactivation was determined with a 50-ms prepulse to –20 mV, a variable recovery interval at a conditioning potential (V_c), then a test pulse to –20 mV. Whole cell currents were filtered at 10 kHz, digitized at 40 kHz, and stored on the fixed drive of a microcomputer (Compaq 386/20). Voltage command pulses were also provided with a microcomputer equipped with a digital-to-analog interface (TL1 interface with Labmaster boards, Axon Instruments, Burlingame, CA).

Single Na⁺ channel currents were measured with 5- to 10-M Ω microelectrodes coated with Sylgard (Dow Corning, Midland, MI) up to the tip. The holding potential was usually set at –100 mV, and 200-ms test pulses were applied to various potentials. In a majority of experiments, test pulses were applied to –20 and –50 mV. Steps to other potentials were applied if the recording condition remained stable. The time dependence of the persistent current was obtained with 200-s depolarizing pulses to potentials of –50 to 0 mV. Currents were filtered at a corner frequency of 2–2.5 kHz by using an eight-pole Bessel filter (model 902 LPF, Frequency Devices, Haverhill, MA). Filtered currents were digitized at 20 kHz.

Data analysis. The procedures for analyzing whole cell and single-channel data are similar to those reported in previous studies from this laboratory (11, 13). Peak currents were measured with custom software written in C programming language. Activation and inactivation were fit with a Boltzmann function (*Eq. 1*) using a Marquardt routine

$$y = 1/[1 + \exp[(V - V_{1/2})/k]] \quad (1)$$

where y is the activation or inactivation variable, V is the membrane potential, $V_{1/2}$ is the potential at which $y = 1/2$, and k is the slope factor. Time constant of recovery from inactivation (τ_{rec}) was obtained from the following equation

$$I_t = I_{\infty}[1 - \exp(-t/\tau_{rec})] \quad (2)$$

where I_t is the peak current at the recovery interval t and I_{∞} is the steady-state current at the test potential. The recovery from inactivation was fit by a single exponential at a recovery potential of –90 mV. The rate of development of inactivation was also fit with a single exponential function.

The residual Na⁺ current at late times was determined from leakage-subtracted currents. Whole cell currents were recorded at high gain using five voltage steps, each of 10–120 mV (in 10-mV increments). The currents for the 10-mV step were averaged, scaled, and subtracted from the current

obtained at other test potentials. Single-channel currents were also leakage and capacity transient subtracted before analysis. Currents during each depolarizing trial were scanned, and those trials without events (nulls) were collected. The nulls were averaged and subtracted from each trial to remove residual leakage and capacity current. In some multichannel patches, no nulls were observed. In those experiments, 20–30 trials with depolarizations of 10 or 20 mV were performed. These trials were scanned, and the nulls were averaged, scaled, and used for leakage and capacity transient subtraction. An automatic detection scheme with the threshold set at 0.5 times the single-channel amplitude was used to identify channel openings. Closed times were determined during segments of current records that had no overlapping events. Less than 12% of trials were excluded because of overlapping events.

Open and closed time histograms were fit with exponentials using a least-squares procedure. The bin width was set at an integer multiple of the sampling interval. Using simulated data from a gating model with known rate constants, we have shown that our fitting technique provides an accurate measure of event distribution (17). Most open times of single Na⁺ channels span a single logarithmic unit. Under these circumstances, logarithmic binning as proposed by Sigworth and Sine (34) provides no advantage over linear binning. Values are means \pm SE. Comparisons were made by unpaired *t*-test or ANOVA. Channel openness during 2-s segments of 200-s depolarizing trials was compared by χ^2 analysis. *P* < 0.05 was considered significant.

RESULTS

Whole cell currents. For the wild-type and Δ KPQ mutant Na⁺ channel, we identified two clones from each construct that expressed robust Na⁺ currents of several nanoamperes. In <5% of untransfected cells we observed endogenous whole cell Na⁺ currents of 10–20 pA. These were not of sufficient amplitude to affect the results reported in this study. Figure 1 illustrates the current-voltage relationship and conductance-voltage and steady-state inactivation curves in cells expressing the wild-type and Δ KPQ mutant Na⁺ channels. Measurable current was observed at –60 mV. There was a gradual rise in current amplitude with increasing

depolarization for both channel types; peak inward current was observed at –20 mV. Potential for half-activation (–37.4 and –37.9 mV) and slope factor (5.8 and 7) were similar for the two channel types. The inactivation curves show a progressive decline in current amplitude as the conditioning potential was reduced. There was no crossover of the current waveform as current amplitude declined. Potentials for half-inactivation were –83.2 and –91.5 mV; slope factors were 6.5 and 5.3 for wild-type and Δ KPQ mutant channels, respectively. Unlike our observations and those of others in native cells, these parameters were stable under the present recording conditions (14). At 15 and 30 min, these parameters were –84.5 mV and 6.4 and –84.9 mV and 6.4, respectively, for the cell expressing the wild-type channel. Similar stability was noted during long recordings from another cell.

Kinetic parameters for activation and inactivation of cells expressing the wild-type and Δ KPQ mutant Na⁺ channel are compared in Table 1. The potential for half-activation is similar to that reported for Na⁺ current recorded from rabbit atrial cells with the perforated-patch technique (40). It is positive to that observed with F[–]-containing micropipette solution in the conventional whole cell configuration (11). The potential for steady-state half-inactivation was similar in wild-type and mutant Na⁺ channels. It was intermediate between that observed with the perforated and conventional whole cell techniques (11, 40). There were clear differences in the kinetics of development of and recovery from inactivation between the wild-type and Δ KPQ mutant Na⁺ channels. At a potential where there was no significant inward current (–80 mV) and at potentials at which there was measurable inward Na⁺ current (–60 and –40 mV), inactivation developed much more rapidly in the Δ KPQ mutant channel. Similarly, the rate of recovery from inactivation at –90 mV was almost twice as fast in the Δ KPQ mutant Na⁺ channel.

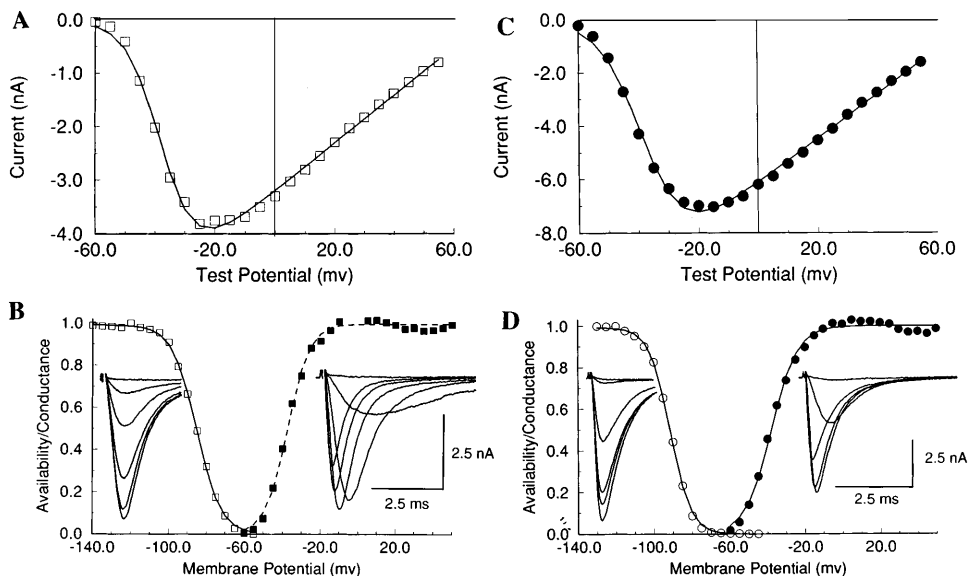


Fig. 1. Whole cell currents in cells expressing wild-type (*A* and *B*) and Δ KPQ mutant α -subunit (*C* and *D*). *A* and *C*: current-voltage relationship obtained with 20-ms pulses from a holding potential of –100 mV. *B* and *D*: conductance-voltage relationships; potentials for half-activation were –37.4 and –37.9 mV, and slope factors were 5.8 and 7. For inactivation curves in *B* and *D*, potentials for half-inactivation were –85.2 and 91.5 mV and slope factors were 6.5 and 5.3. Representative current records obtained with activation and inactivation protocols are also shown in *B* and *D* (insets). *A*: \square , peak currents as function of test potential. *B*: \square and \blacksquare , inactivation and activation curves, respectively. *C*: \bullet , peak currents of KPQ deletion mutant channel. *D*: \circ and \bullet , inactivation and activation curves, respectively.

Table 1. Comparison of gating parameters of wild-type and Δ KPQ mutant Na⁺ channels

	Wild Type	Δ KPQ
<i>Activation</i>		
$V_{1/2}$, mV	-32.5 ± 6.3 (7)	-30.6 ± 3.5 (6)
k	7.2 ± 0.3	6.3 ± 0.4
<i>Inactivation</i>		
$V_{1/2}$, mV	-84.9 ± 1.3	-86.5 ± 2
k	6.5 ± 0.3	6.7 ± 0.5
<i>Development of inactivation</i>		
τ_c , -40 mV, ms	2 ± 0.3 (9)	0.7 ± 0.07 (5)
τ_c , -60 mV, ms	12.3 ± 2.6 (9)	2.6 ± 0.6 (4)
τ_c , -80 mV, ms	55 ± 9 (9)	14.5 ± 1.7 (6)
<i>Recovery from inactivation</i>		
τ , -90 mV, ms	28.5 ± 1.4 (5)	18 ± 1.4 (5)

Values are means \pm SE of number of observations in parentheses. $V_{1/2}$, potential at which y (activation or inactivation variable) = 1/2; k , slope factor; τ_c , time constant.

Figure 2 compares inactivation of the macroscopic current in wild-type and mutant Na⁺ channels. Figure 2, A and B, shows currents in response to test pulses from -100 to -40 mV. For cells expressing each channel type, the relaxation of the current was well fit by single exponentials. The time constants (τ_c) for wild-type and Δ KPQ mutant currents were 3.1 and 1.6 ms, respectively. Summary data are presented in Fig. 2C. Between -50 and +40 mV, τ_c decreased sevenfold for the wild-type channel. In contrast, τ_c for the Δ KPQ mutant channel was weakly voltage dependent, decreasing only 1.7-fold over the same voltage range.

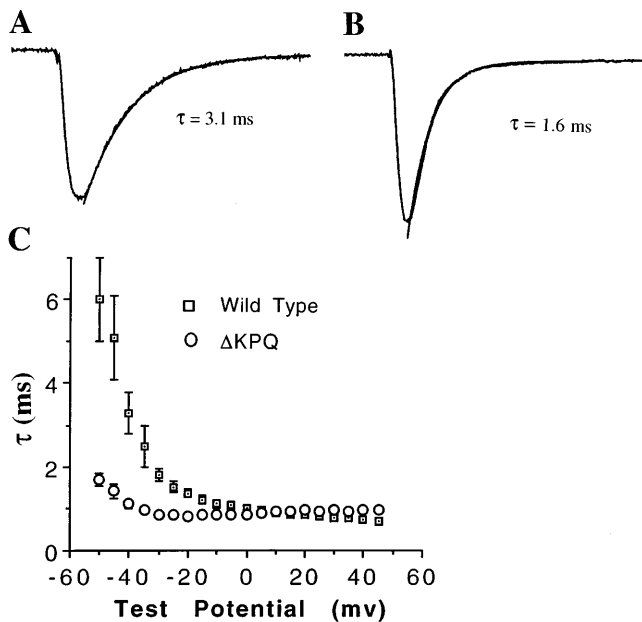


Fig. 2. Kinetics of inactivation of whole cell current in wild-type and Δ KPQ mutant Na⁺ channels. A and B: whole cell Na⁺ currents elicited with pulses to -40 mV from a holding potential of -100 mV in cells expressing wild-type and Δ KPQ mutant Na⁺ channels. Relaxation phase of currents was fit with single exponentials. C: average time constant plotted as a function of test potential.

Despite the appearance of faster inactivation of the whole cell currents, a persistent component of Na⁺ current was observed in the HEK293 cells expressing the Δ KPQ mutant. Figure 3 shows leakage-subtracted Na⁺ currents recorded at high gain (A) and Na⁺ current recorded at a lower gain (B) from the same cell. Holding and test potentials were -100 and -20 mV, respectively. The initial transient of inward current saturated the amplifier when recorded at high gain. At the end of the 200-ms pulse, inward current of amplitude 1% that of the peak current persisted. In the last 50 ms of the pulse, there was no perceptible time-dependent change of the current. The initial transient and persistent current were normalized to the current at -20 mV and plotted against test voltage in Fig. 3C. The amplitude of the persistent current paralleled that of the peak current, suggesting that the persistent current results from a transient change in gating of a fraction of the channels. This result contrasts with that observed for the transient and persistent Na⁺ current in rat ventricular myocytes in which the current-voltage relationship of the persistent current is shifted to more negative potentials by \sim 20 mV (31).

Single-channel recordings. We examined the bases for some of these changes observed at the whole cell level by recording single-channel Na⁺ current in the

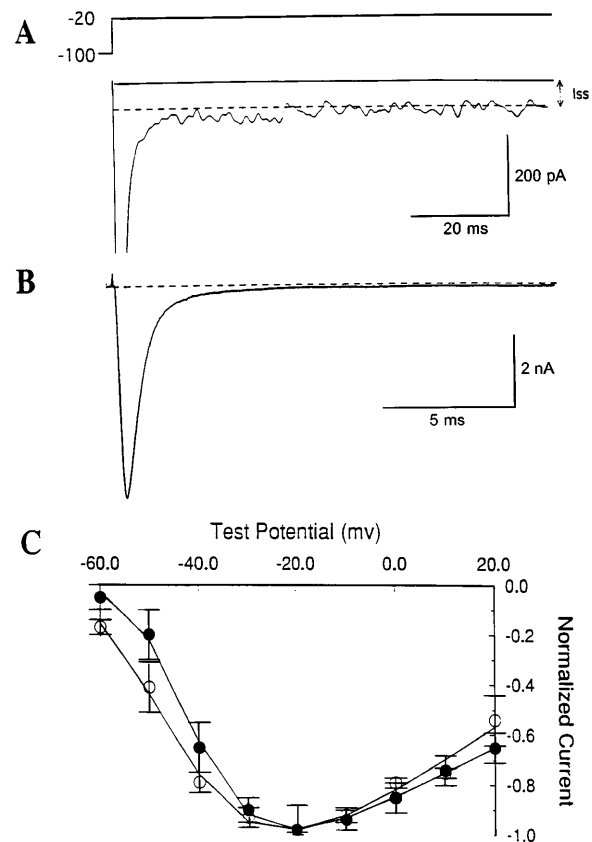


Fig. 3. Late component of current in a cell expressing Δ KPQ mutant Na⁺ channel. A and B: leakage-subtracted whole Na⁺ current elicited by a 200-ms test pulse to -20 mV from a holding potential of -100 mV. Initial surge of Na⁺ current saturated amplifier. I_{ss} , steady-state current at end of 200-ms pulse. C: \bullet , initial Na⁺ current as function of test potential; \circ , steady-state current as function of test potential.

cell-attached configuration. Depending on the choice of microelectrode tip size and the density of channels in the cell, we were able to record from patches that contained a few or many Na⁺ channels. For detailed kinetic analysis during step depolarizations, we used patches that contained a few Na⁺ channels. Figure 4 compares membrane currents recorded during 10 consecutive voltage steps from -100 to -40 mV in cells expressing the wild-type and Δ KPQ mutant Na⁺ channels. The maximum number of overlapping events suggests that there were at least three functioning channels in the patch for the wild-type channel. Channel openings occurred after a brief latency and consisted predominantly of single or overlapping openings having a mean open time of 1 ms. At later times, e.g., in the first trial, occasional openings were observed. There was evidence for three functioning channels in the patch containing the Δ KPQ mutant. The initial channel openings of 0.9-ms mean duration also occurred after a brief latency. However, late openings were observed in many trials. As was observed in frog oocytes, these took the form of isolated brief background openings and bursts of openings. The fifth trial shows an isolated brief opening late in the trial without a preceding early opening. This suggests that a closed channel may have passed directly to the inactivated state but visited the open state by a return from inactivation. The trials containing bursts tended to cluster, suggesting that the channels functioned in a

distinct mode for a period of time well beyond the interpulse interval (1,000 ms). The probability that a channel would fail to open at late times (P_{fi}) was estimated from the n th root of the fraction of trials with no openings after 20 ms, where n is the number of channels in the patch and is estimated from the maximum number of overlapping openings during the initial transient. The complement of P_{fi} is the probability that a channel will open after 20 ms. These probabilities were 0.01 and 0.22 for the wild-type and mutant channels in Fig. 4. The estimates should be regarded as the upper limit of the probabilities, because the number of channels in the patch is likely to have been underestimated. The averaged current in the lowest trace of Fig. 4 shows that those late openings summed to produce a persistent component of inward current. The persistent current amounted to 4% of the peak current. The two forms of late openings are similar to those originally described in cardiac and skeletal muscle by Patlak and Ortiz (28, 29).

To clarify whether there were indeed two modes of gating at late times, we examined the voltage dependence of the isolated brief openings and bursts recorded from a single patch with the Δ KPQ mutant (Fig. 5). Each trial was arbitrarily divided into an early segment (0–20 ms) and a late segment (20–200 ms). Twenty milliseconds should be sufficient for the initial transient to reach steady state, inasmuch as the time

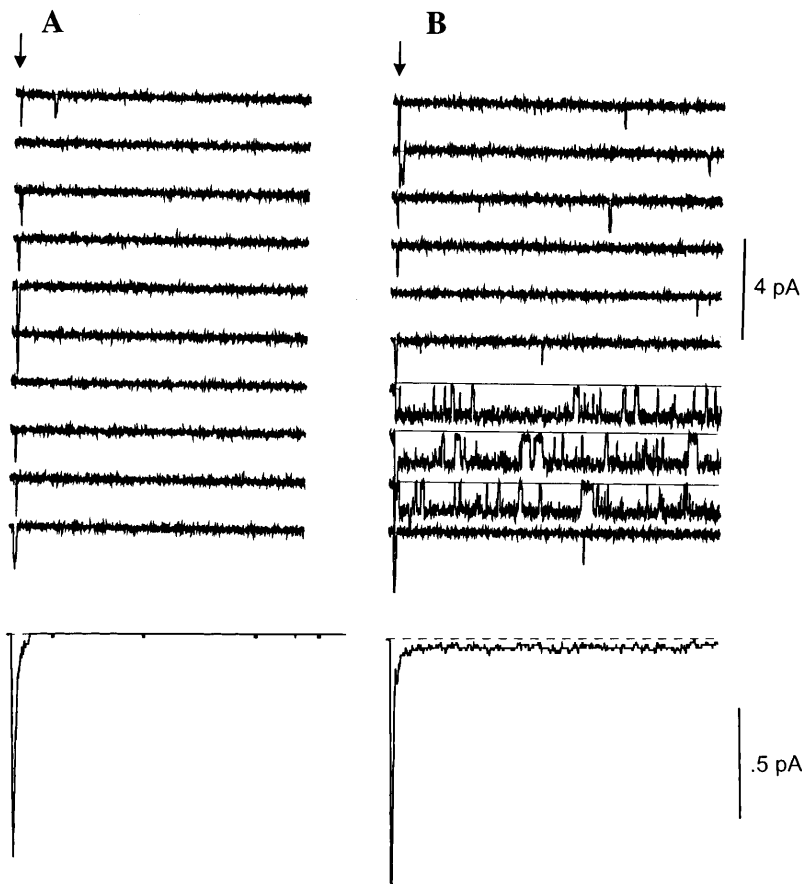
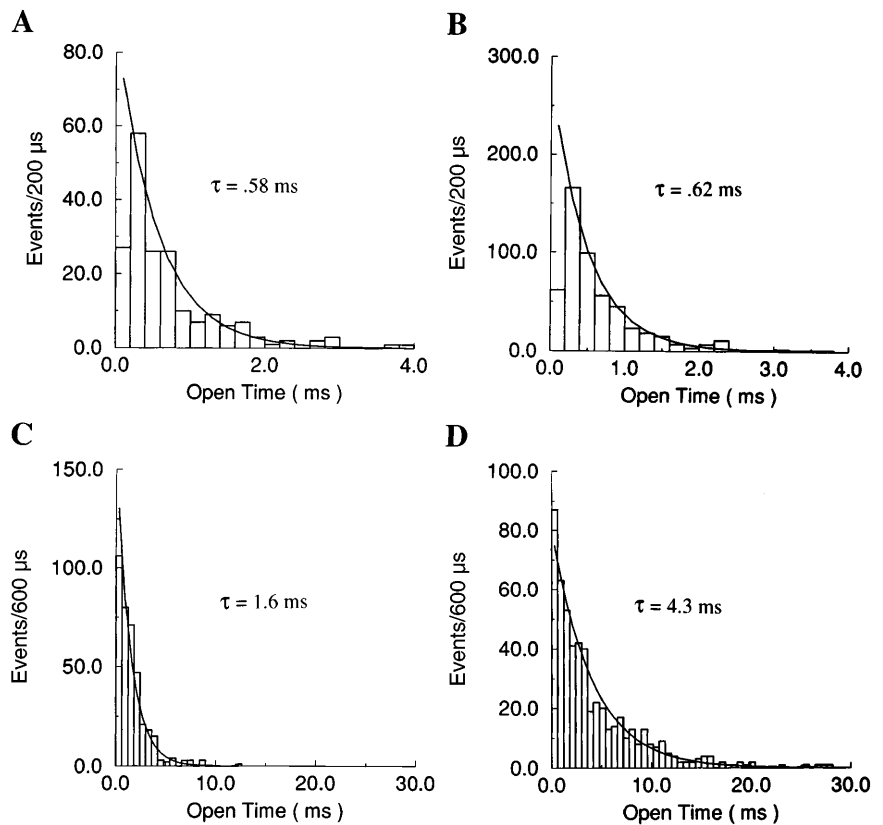


Fig. 4. Single Na⁺ current recorded from cells expressing wild-type (A) and Δ KPQ mutant (B) Na⁺ channel. Currents elicited during 10 consecutive depolarizing trials are shown; averaged current is shown in lowest trace. Dashed line, zero current level for averaged current traces. Vertical arrows, onset of depolarization. Membrane currents were obtained in cell-attached configuration with 200-ms depolarizing pulses from -100 to -40 mV.

Fig. 5. Comparison of voltage dependence of distribution of open times during isolated openings (A and B) and bursts (C and D). Histograms of distribution of open times during isolated openings and bursts were compiled from depolarizing trials to -50 (A and C) and -20 mV (B and D) in a single patch. At each potential, distribution of open times was fit with a single exponential. Closing time constant (τ) of isolated openings showed little voltage dependence, whereas that of bursts increased ~ 2.7 -fold with depolarization between -50 and -20 mV.



constant of macroscopic inactivation was <3 ms at all test potentials. At each potential the distribution of open times was well fit with a single exponential. For the isolated brief openings, mean open times were 0.58 and 0.62 ms at test potentials of -50 and -20 mV, respectively. In contrast, the mean open time during the burst increased 2.7-fold over the same range of membrane potential. Summary data over a range of membrane potential are presented in Fig. 6. Whereas mean open times for the isolated opening showed little voltage dependence, those during the bursts increased progressively with membrane depolarization.

We examined whether the closing mechanisms for the initial transient and the isolated brief openings occurring at late times were the same by comparing the open times. Trials with bursts were excluded from this analysis, inasmuch as we now postulate that closing during the bursts is controlled by a different mechanism. Mean open times at early and late times are compared in Fig. 7. The mean open times at early and late times were not significantly different. The trend for the open times of the early events to be longer could have resulted from the error introduced by the presence of overlapping events.

The distribution of closed times during bursts and the brief late openings may provide insight into the opening mechanisms occurring at late times. Unfortunately, the distribution of closed times can be readily interpreted only when a single ion channel is contributing to the ensemble. The patches observed during these experiments were usually multichannel, making them less than ideal for analysis of the closed time distribu-

tion. However, the occurrence of prolonged bursts without overlapping events suggests, with a high degree of certainty, that a single channel is contributing to such activity. Figure 8 shows single-channel current in eight consecutive trials during recording from a membrane patch expressing the Δ KPQ mutant. The holding and

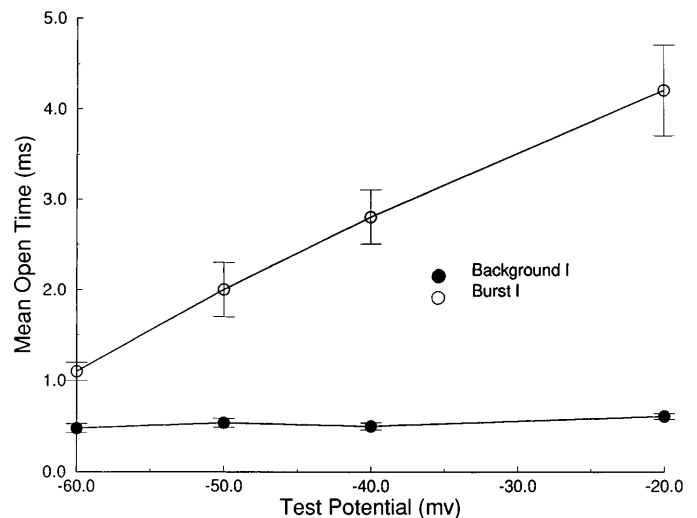


Fig. 6. Summary of voltage dependence of mean open times of isolated opening and bursts of openings. Ordinate, open times (means \pm SE of 4–5 experiments); abscissa, test potential. \bullet , Means of isolated openings; \circ , means of bursts. Equivalent charge movement for Na⁺ channel closure during burst was 0.8 electronic charges (calculated from $\ln(1/\tau_0)/dV$, where τ_0 is mean open time and V is membrane potential). All data were obtained in membrane patches from cells expressing Δ KPQ mutation.

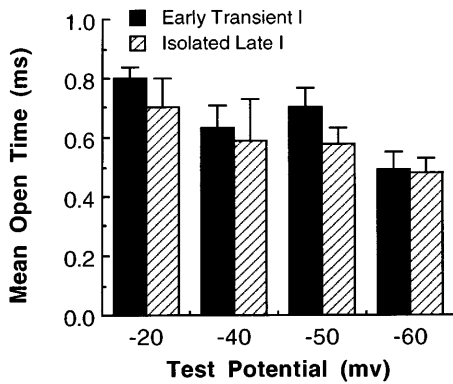


Fig. 7. Comparison of mean open time of early and late current in cells expressing Δ KPQ mutant Na⁺ channel. Each depolarization was arbitrarily divided into early (0–20 ms) and late (20–200 ms) segments. Mean open times at early and late times were not significantly different.

test potentials were –100 and –50 mV, respectively. The analysis of consecutive bursts provides a large number of events for kinetic analysis, yet the heterogeneity associated with bursting in different patches should be reduced. The records imply a complex gating mechanism during bursts. Channel openings are interrupted by brief closures, many of which are not well resolved. Longer closures separate groups of openings. The histogram of the distribution of closed times is well fit by two exponentials, with time constants of 0.22 and 1 ms. For illustrative purposes, the histogram was truncated at 7.5 ms. Occasional events exceed this limit. However, there were insufficient long-lasting events to attempt a higher-order (i.e., 3) exponential fit. When data from other patches with few bursts were combined at each test potential, multiple exponentials were usually required to fit the histogram of closed times.

The closed times between brief late openings were more difficult to interpret. Patlak and Ortiz (29) also observed a biexponential distribution for these events and suggested that the short time constants reflected reopenings of the same channel. This interpretation is not applicable to the late currents observed with the

Δ KPQ mutant. For patches with one or two active channels, a majority of late openings were single isolated events occurring during the 200-ms depolarizing trials (Fig. 4). Closely spaced openings during 200-ms trials or constant depolarization (see Fig. 10, insets) are likely to be the result of opening of separate channels. The closed times between such openings are not informative.

We examined the time dependence of the persistent current by applying a steady holding potential for 200 s. Data acquisition was interrupted every 200 ms for a period of 1 ms to reset the buffers. Data from an illustrative experiment are presented in Fig. 9. The holding potential was –20 mV. Channel “openness” was quite variable over the 200-s interval. A χ^2 analysis suggested that the 200-ms segments were not homogeneous. However, there was no tendency for the total current to decrease at late times. Occasional long openings were observed during steady depolarization. However, they were isolated (e.g., segment B) rather than occurring in bursts. When the distribution of open times of all events observed during steady depolarization was compared, the open times followed a single distribution. As illustrated in Fig. 10, their mean open time and lack of voltage dependence suggest that the openings during steady depolarization reflect the isolated openings.

We used single-channel recordings to examine the basis of much faster rates of current relaxation in the Δ KPQ mutant channels. At potentials close to threshold, the macroscopic inactivation is dominated by the first latency distribution. At these potentials, opening probability is low. Therefore, a large number of trials is required to estimate the first latency distribution. Figure 11 shows cumulative first latencies in single patches, each expressing the wild-type and Δ KPQ mutant Na⁺ channels. The cumulative probabilities are conditional that a channel opened (nulls were omitted). Data are based on 550 trials of the wild-type channel and 996 trials of the Δ KPQ mutant channels during step depolarizations from –100 to –50 mV. Mean open

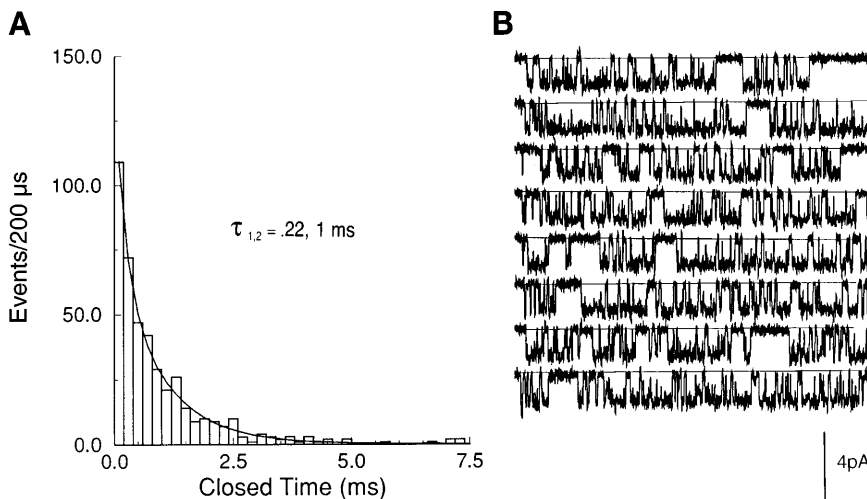
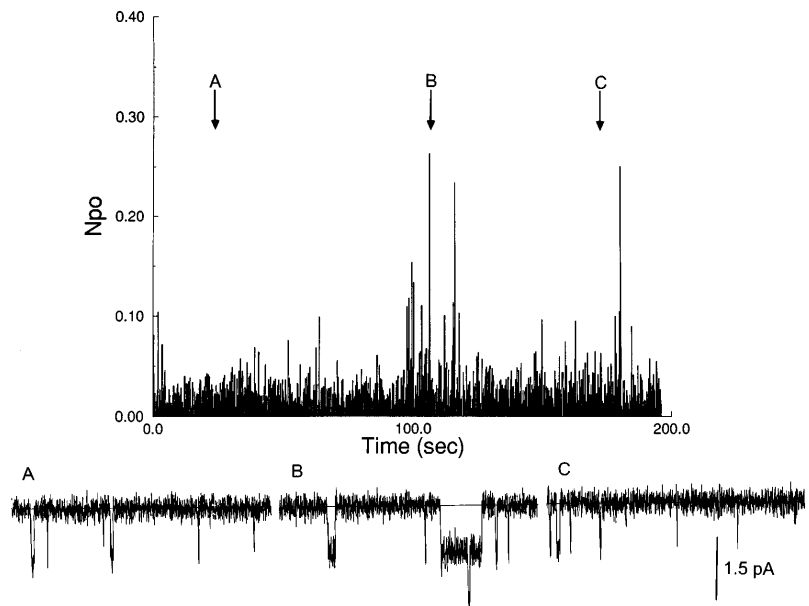


Fig. 8. A: distribution of closed times during bursts of Δ KPQ mutant Na⁺ channels. B: current records showing membrane currents during 8 consecutive trials of an ensemble of 489 trials. Currents were elicited by 200-ms pulses from a holding potential of –100 to –50 mV. Histogram of closed times was fit with 2 exponentials, with time constants (τ_1 and τ_2) of 0.22 and 1 ms.

Fig. 9. *Top*: time dependence of late current during steady depolarization. Membrane currents were recorded from a cell-attached membrane patch with a low-resistance microelectrode. Holding potential was maintained for 200 s. Ordinate, channel openness [NP_o , i.e., product of number of channels in patch (N) and probability of a channel being open (P_o) during 200-ms segments]; abscissa, time. *Bottom*: expanded time scale; 200-ms segments obtained early and late during 200-s depolarization (*A* and *C*), together with a high open probability (P_o) segment (*B*).



times of the wild-type and ΔKPQ mutant channels were 0.6 ± 0.6 and 0.8 ± 1 ms, respectively. The first latency distribution of the wild-type channel took a simple form. The first 10 ms was fit by a single exponential with a time constant of 3.1 ms. The cumulative distribution of the ΔKPQ mutant took a more complex form. After an initial rapid rise, there was a slow progressive tail, reflecting first openings occurring at late times. The initial 10-ms period was fit by a double exponential with time constants of 0.6 and 25 ms. These data suggest that early openings occur faster in the ΔKPQ mutant channel.

DISCUSSION

Initial transient current. We have used whole cell and single-channel recordings to determine the changes in kinetics of the Na^+ channel that result from the KPQ deletion. Experiments were performed in HEK cells. These cells have diameters of ≤ 10 μm and readily formed gigaohm seals with microelectrodes of ~ 1 M Ω resistance. In 130 mM external Na^+ , the Na^+ current was usually well controlled, as judged by the slope factor of the activation curve and the lack of overlap of the current waveform as the current amplitude was reduced with the inactivation voltage-clamp protocol (11). Voltage dependence of steady-state activation and inactivation were stable during prolonged recordings from these cells.

The rate of onset and of recovery of inactivation were accelerated by the KPQ deletion. Because both kinetic parameters were increased, we did not observe a significant shift in the voltage dependence of inactivation. Bennett et al. (6) first reported the effects of the KPQ deletion on the kinetics of inactivation of Na^+ channels expressed in frog oocytes. They observed a 6-mV negative shift in the potential for half-inactivation of the ΔKPQ mutant. The rate of recovery from inactivation was unchanged. Presumably, β_h , the rate constant for

the onset of inactivation, must have increased. However, this parameter was not reported. An et al. (3) examined the kinetics of inactivation of ΔKPQ mutant Na^+ channels expressed in HEK cells. As reported in the present study, they also observed an acceleration in the rate of recovery from inactivation. The difference in the kinetics of recovery in frog oocytes and HEK cells may reflect the presence of regulatory subunits in the latter cell type.

As has been reported in two earlier studies, we observed an acceleration of the rate of macroscopic inactivation (6, 10). The effect was most marked around the threshold for measurable inward current at about -50 mV. The faster relaxation of the current could have resulted from a decrease in mean open time or of latency to first opening. We did not observe a significant change in mean open time at -50 mV. In fact, in the experiment illustrated in Fig. 11, mean open time was longer in the ΔKPQ mutant channel (0.8 vs. 0.6 ms). The studies of Aldrich et al. (1, 2) emphasize the importance of the first latency in determining the relaxation of the macroscopic current at a neuronal Na^+ channel. This factor is also important in cardiac muscle for small depolarization. Latency to first opening was changed by the mutation. An initial early component was accelerated, and a later component reflected the occurrence of isolated brief openings without earlier openings. Such opening may reflect direct passage of closed channels to the inactivated state and a later brief visit to the open state. The acceleration of the rate of development of inactivation at -80 mV supports an increased rate of inactivation of closed channels. The acceleration of the initial component of the first latency suggests an acceleration of the rate of activation by the ΔKPQ mutation. Inasmuch as this mutation affects a segment of the Na^+ channel usually associated with inactivation, the two processes may be coupled. These results are consistent with those of

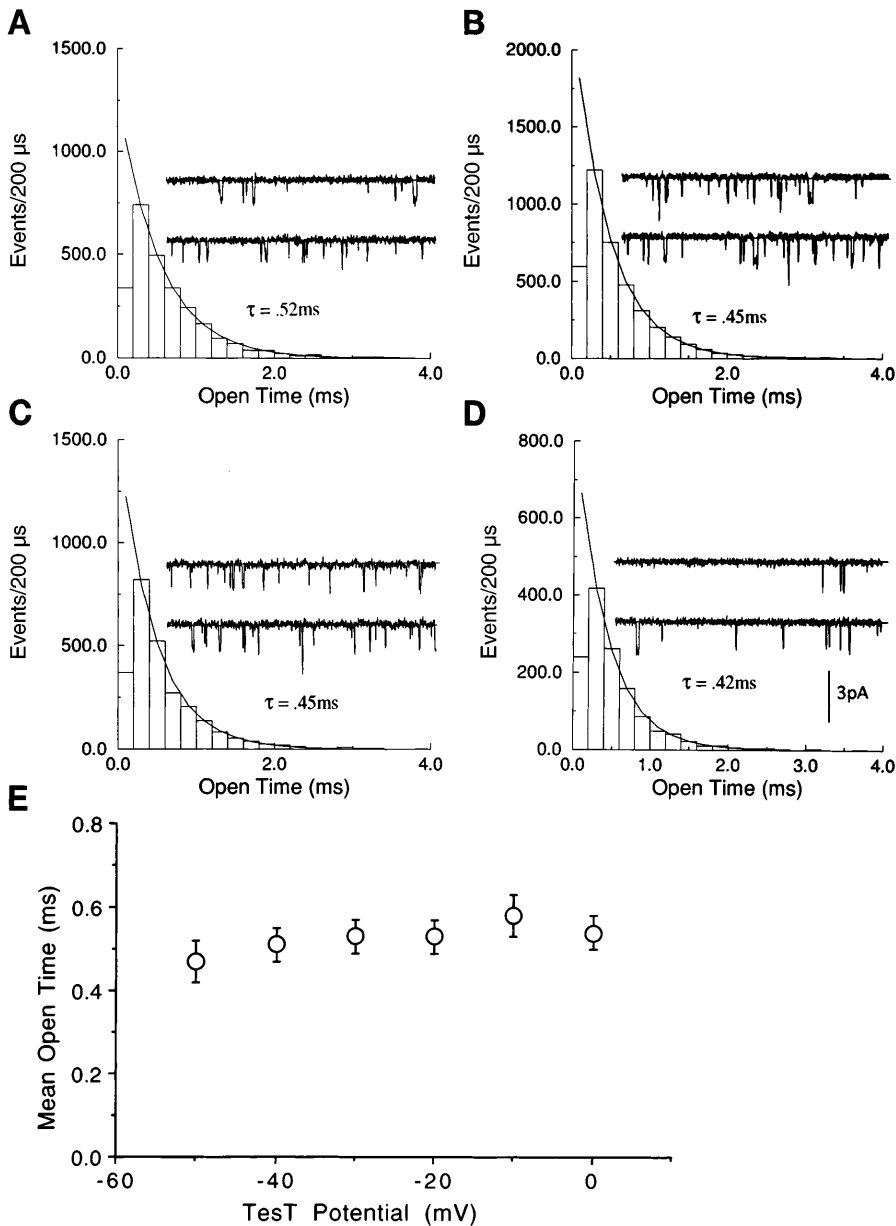


Fig. 10. Voltage dependence of distribution of open times of isolated openings observed during steady depolarization. A–D: histograms and two 200-ms segments of records obtained during steady depolarization at –10 (A), –20 (B), –30 (C), and –40 mV (D). At each potential, histogram was fit by a single exponential. E: average data from 4–9 experiments.

O’Leary et al. (27). They showed that when vicinal Tyr-1494 and -1495, located between the IFM and Δ KPQ residues, were mutated to Gln (YY/QQ), macroscopic inactivation is accelerated for small depolarizations and latency to first opening is shortened.

Late components of Na⁺ current. The nature of the late component of Na⁺ current in the Δ KPQ mutant is controversial. Bennett et al. (6) observed that the late openings result from a modal shift to a single bursting state. On the other hand, Dumaine et al. (10) observed two modes of gating in cell-attached patches in frog oocytes. We examined the voltage and time dependence of the late Na⁺ channel current at the single-channel level in cell-attached recordings. Our results are consistent with two modes of gating at late times: isolated brief openings and bursts of opening. The open times of the isolated openings were weakly voltage dependent. They were of the same duration as the open times of the

events that make up the early transient current. The simplest explanation for these openings is that they result from an increase in the reversibility of fast inactivation (10). Wild-type Na⁺ channels open once at most depolarized potentials; i.e., the fast inactivated state is absorbing. The Δ KPQ mutant Na⁺ channels return from the fast inactivated state at a slow but significant rate. Inasmuch as the closure mechanisms are postulated to be without memory, the late openings should close at the same rate as those during the early transient.

When examined over a wide range of voltages, Na⁺ channel open times show significant voltage dependence, with a critical value at –30 to –10 mV and a decline around threshold and at strongly depolarized potentials (42). However, special recording conditions, e.g., high external Na⁺ concentration, are required to obtain accurate kinetics at the extremes of voltages.

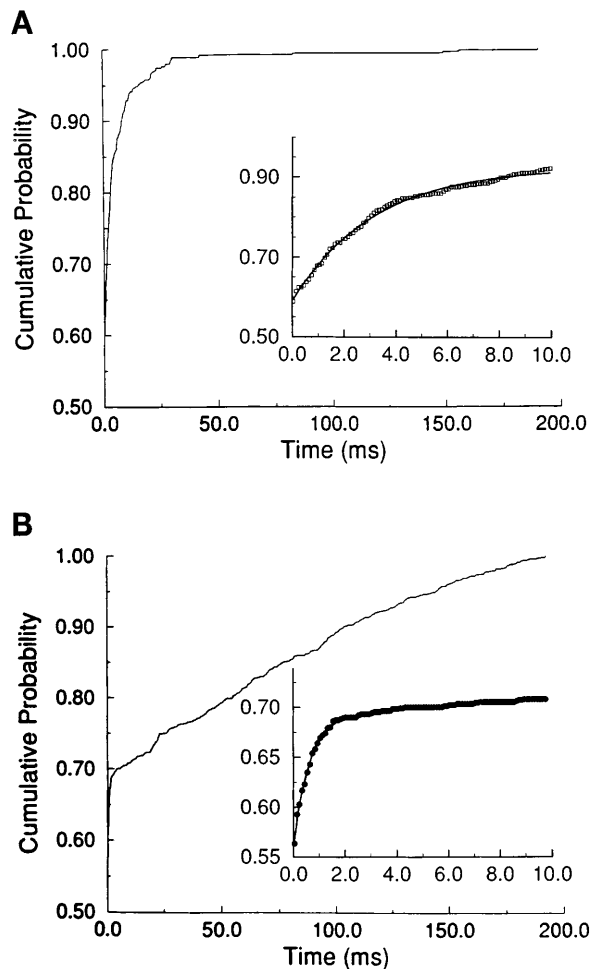


Fig. 11. Cumulative latency to first opening in membrane patches expressing wild-type (A) and Δ KPQ mutant (B) Na⁺ channels. Cumulative probability of first opening is plotted against time after onset of depolarization. *Insets*: first 10 ms of each distribution plotted on an expanded scale. Probabilities are conditional on ≥ 1 opening occurring in a trial. Data are based on ensembles of 550 trials in a patch with wild-type channels and 996 trials in a patch with Δ KPQ mutant channels. Holding potential, -100 mV; test potential, -50 mV.

Over the limited range of voltage studied, our results are consistent with the earlier studies of voltage dependence of open times.

The persistence of the isolated brief openings when depolarization is maintained for as much as 200 s suggests that the channels are not undergoing slow inactivation. However, there are a number of other possibilities. At the voltages tested, slow inactivation may not be complete; i.e., at equilibrium, there may be significant occupancy in the fast inactivated state. Clarkson et al. (8) reported steady-state values of slow inactivation of ~ 0.5 s in the 0- to -60 -mV range of membrane potentials. An alternative possibility is that the Δ KPQ mutation may have also modified the kinetics of slow inactivation (10).

In contrast to the isolated openings, the mean open times of the bursts were strongly voltage dependent. They increased 2.7-fold over a 40-mV range of membrane potential. In the wild-type channels, Patlak and Ortiz (29) proposed that bursts result from a transient

failure of fast inactivation. The Na⁺ channel kinetics are then reduced to the simple form



where C_n are the closed states preceding opening, O is the open state, α_m is the activation rate constant, and β_m is the deactivation rate constant. Channels closed by deactivation with a mean open time τ_o are given as follows

$$1/\tau_o = 3\beta_m \quad (4)$$

From the voltage dependence of the mean open times during the bursts, we calculated a valency of 0.8 electronic charges for the deactivation transition. This is of the same order of magnitude as that estimated by Yue et al. (42) for the deactivation of wild-type Na⁺ channels in native membranes. A similar analysis of the early transient of the Δ KPQ mutant is not possible, inasmuch as the analysis is critically dependent on the assumption that fast inactivation is absorbing (1).

The kinetic scheme outlined in Eq. 3 indicates that the distribution of closed times should reflect the kinetics of activation. A fit to the distribution of closed times required at least two exponentials. The rate constants of these exponentials do not reflect the elemental rate constant α_m and $2\alpha_m$, but the eigenvalues of the submatrix describing the transitions to the open state. The short time constant is of the same order of magnitude as the short time constant of the first latency distribution. At room temperature the rising phase of the macroscopic current was not sufficiently resolved to fit multiple exponentials to it. Therefore, the closed time constant could not be compared with the time constants of the rising phase of the macroscopic current.

The two modes of gating observed at late times with the KPQ deletion mutant are qualitatively similar to that observed in native cardiac cells. The reduction in the action potential duration by tetrodotoxin and Na⁺ channel-blocking antiarrhythmic drugs supports the presence of a slow component of Na⁺ current in cardiac cells (9, 39). Single-channel recordings have identified both forms of late gating in ventricular and Purkinje cells (12, 19, 28). The KPQ deletion increases the likelihood of the slow gating mechanism.

Implications of the changes in Na⁺ channel gating. This study extends the earlier analysis of Bennett et al. (6), Dumaine et al. (10), and An et al. (3) in defining the voltage and time dependence of gating of the KPQ deletion mutant Na⁺ channel. These studies provide a basis for the prolongation of the Q-T interval on the surface ECG. We explored the impact of the changes in kinetics of the Na⁺ current on membrane excitability. The model of the cardiac action potential recently developed by Luo and Rudy (23) does not include the late component exhibited by wild-type and mutant Na⁺ channels. We varied the noninactivating component of Na⁺ current in the model of Beeler and Reuter (5) and

examined its impact on the action potential. There was a very narrow range of conductance in which the noninactivating Na⁺ current resulted in marked increases in action potential duration and early afterdepolarizations. For example, with a peak conductance of 4 mS and zero noninactivating current, the resulting action potential duration was 290 ms. For a noninactivating Na⁺ current of 0.038 mS (<1% of peak Na⁺ conductance), the action potential duration increased to 670 ms with early afterdepolarizations. Further increases in the noninactivating current resulted in a sustained plateau. Acceleration of the recovery of the Na⁺ channel from inactivation may also increase the window of vulnerability during phase 3 of the action potential. Smith et al. (35) suggested that the large current tail observed in cells expressing the human *ether-á-go-go* (HERG) cardiac K⁺ channel would decrease excitability during phase 3. By diminishing the magnitude of this current, the HERG-associated mutations may enhance excitability during phase 3. The occurrence of persistent inward Na⁺ current at hyperpolarized potentials may also lower the threshold for excitability.

Prolongation of the Q-T interval on the surface ECG is a relatively common observation. However, its association with torsade de pointes is uncommon. Enhanced excitability during phase 3 is a potential mechanism by which the long Q-T interval-associated Na⁺ and K⁺ channel mutations lead to torsade de pointes.

The acceleration of the onset of activation observed in the present study further supports coupling between the activation and inactivation mechanisms. The S4 segment of each domain of the Na⁺ channel is thought to play a critical role in activation. A change in activation after a mutation in the linker between domains III and IV suggests that significant change in the relative positions of the neighboring S4 segments and the III-IV linker may occur during channel gating. The region of the KPQ deletion has multiple Pro residues. Their relatively rigid structure may form a pivot around which some intramolecular movement may occur. The examination of other mutations in this region of the Na⁺ channel may provide further insight into the basis for the coupling of activation and inactivation.

Our preliminary results have been published in abstract form (7).

Address for reprint requests: A. O. Grant, Duke University Medical Center, Box 3504, Durham, NC 27710-3504.

Received 2 September 1997; accepted in final form 4 February 1998.

REFERENCES

1. Aldrich, R. W., D. P. Corey, and C. F. Stevens. A reinterpretation of mammalian sodium channel gating based on single channel recording. *Nature* 306: 436–441, 1983.
2. Aldrich, R. W., and C. F. Stevens. Voltage-dependent gating of single sodium channels from mammalian neuroblastoma cells. *J. Neurosci.* 7: 418–431, 1987.
3. An, R.-H., R. Bangalore, and R. S. Kass. Lidocaine block of LQT-3 mutant human Na⁺ channels. *Circ. Res.* 79: 103–108, 1996.
4. Armstrong, C. M., and R. H. Chow. Supercharging: a method for improving patch-clamp performance. *Biophys. J.* 52: 133–136, 1987.
5. Beeler, G. W., and H. Reuter. Reconstruction of the action potential of ventricular myocardial fibres. *J. Physiol. (Lond.)* 268: 177–210, 1977.
6. Bennett, P. B., K. Yazawa, N. Makita, and A. L. George, Jr. Molecular mechanism for an inherited cardiac arrhythmia. *Nature* 376: 683–685, 1995.
7. Chandra, R., C. F. Starmer, and A. O. Grant. Multiple effects of the delta KPQ mutant on the gating of human cardiac sodium channels expressed in mammalian cells (Abstract). *Circulation* 94, Suppl. I: I-287, 1996.
8. Clarkson, C. W., T. Matsubara, and L. M. Hondeghem. Slow inactivation of V_{max} in guinea pig ventricular myocardium. *Am. J. Physiol.* 247 (Heart Circ. Physiol. 16): H645–H654, 1984.
9. Coraboeuf, E., E. Deroubaix, and A. Coulombe. Effects of tetrodotoxin on action potentials of the conducting system in dog heart. *Am. J. Physiol.* 236 (Heart Circ. Physiol. 5): H561–H567, 1979.
10. Dumaine, R., Q. Wang, M. T. Keating, H. A. Hartmann, P. J. Schwartz, A. M. Brown, and G. E. Kirsch. Multiple mechanisms of Na⁺ channel-linked long-QT syndrome. *Circ. Res.* 78: 916–924, 1996.
11. Gilliam, F. R., III, C. F. Starmer, and A. O. Grant. Blockade of rabbit atrial sodium channels by lidocaine: characterization of continuous and frequency-dependent blocking. *Circ. Res.* 65: 723–739, 1989.
12. Grant, A. O., F. R. Gilliam III, M. Dietz, and C. F. Starmer. Slow gating kinetics of cardiac sodium channels in rabbit Purkinje cells (Abstract). *Circulation* 78, Suppl. II: 410, 1988.
13. Grant, A. O., and C. F. Starmer. Mechanisms of closure of cardiac sodium channels in rabbit ventricular myocytes: single-channel analysis. *Circ. Res.* 60: 897–913, 1987.
14. Hanck, D. A., and M. F. Sheets. Time-dependent changes in the kinetics of sodium current in single canine cardiac Purkinje cells. *Am. J. Physiol.* 262 (Heart Circ. Physiol. 31): H1197–H1207, 1992.
15. Hartmann, H. A., A. A. Tiedeman, S.-F. Chen, A. M. Brown, and G. E. Kirsch. Effects of III-IV linker mutations on human heart Na⁺ channel inactivation gating. *Circ. Res.* 75: 114–122, 1994.
16. Higuchi, R. Recombinant PCR. In: *PCR Protocols: A Guide to Methods and Applications*. San Diego, CA: Academic, 1990, p. 177–183.
17. Hurwitz, J. L., M. A. Dietz, C. F. Starmer, and A. O. Grant. A source of bias in the analysis of single channel data: assessing the apparent interaction between channel proteins. *Comput. Biomed. Res.* 24: 584–602, 1991.
18. Isom, L. L., K. S. De Jongh, D. E. Patton, B. F. X. Reber, J. Oxford, H. Charbonneau, K. Walsh, A. L. Goldin, and W. A. Catterall. Primary structure and functional expression of the β_1 subunit of the rat brain sodium channel. *Science* 256: 839–842, 1992.
19. Kiyosue, T., and M. Arita. Late sodium current and its contribution to action potential configuration in guinea pig ventricular myocytes. *Circ. Res.* 64: 389–397, 1989.
20. Krafte, D. S., A. L. Goldin, V. J. Auld, R. J. Dunn, N. Davidson, and H. A. Lester. Inactivation of cloned Na channels expressed in *Xenopus* oocytes. *J. Gen. Physiol.* 96: 689–706, 1990.
21. Krafte, D. S., and H. A. Lester. Expression of functional sodium channels in stage II-III *Xenopus* oocytes. *J. Neurosci. Methods* 26: 211–215, 1989.
22. Krafte, D. S., T. P. Snutch, J. P. Leonard, N. Davidson, and H. A. Lester. Evidence for the involvement of more than one mRNA species in controlling the inactivation process of rat and rabbit brain Na channels expressed in *Xenopus* oocytes. *J. Neurosci.* 8: 2859–2868, 1988.
23. Luo, C.-H., and Y. Rudy. A dynamic model of the cardiac ventricular action potential. *Circ. Res.* 74: 1071–1096, 1994.
24. Makita, N., Jr., P. B. Bennett, and A. L. George, Jr. Voltage-gated Na⁺ channel β_1 subunit mRNA expressed in adult human skeletal muscle, heart and brain is encoded by a single gene. *J. Biol. Chem.* 269: 7571–7578, 1994.

25. **Methfessel, C., V. Witzemann, T. Takahashi, M. Mishina, S. Numa, and B. Sakmann.** Patch-clamp measurements on *Xenopus laevis* oocytes: currents through endogenous channels and implanted acetylcholine receptor and sodium channels. *Pflügers Arch.* 407: 577–588, 1986.
26. **Nuss, H. B., N. Chiamvimonvat, M. T. Perez-Garcia, G. F. Tomaselli, and E. Marban.** Functional association of the β_1 -subunit with human cardiac (hH1) and rat skeletal muscle (ml) sodium channel α subunits expressed in *Xenopus* oocytes. *J. Gen. Physiol.* 106: 1171–1191, 1995.
27. **O'Leary, M. E., L.-Q. Chen, R. G. Kallen, and R. Horn.** A molecular link between activation and inactivation of sodium channels. *J. Gen. Physiol.* 106: 641–658, 1995.
28. **Patlak, J. B., and M. Ortiz.** Slow currents through single sodium channels of adult rat heart. *J. Gen. Physiol.* 86: 89–104, 1985.
29. **Patlak, J. B., and M. Ortiz.** Two modes of gating during late Na⁺ channel currents in frog sartorius muscle. *J. Gen. Physiol.* 87: 305–326, 1986.
30. **Patton, D. E., J. W. West, W. A. Catterall, and A. L. Goldin.** Amino acid residues required for fast Na⁺-channel inactivation: charge neutralizations and deletions in the III-IV linker. *Proc. Natl. Acad. Sci. USA* 89: 10905–10909, 1992.
31. **Saint, D. A., Y. K. Ju, and P. W. Gage.** A persistent sodium current in rat ventricular myocytes. *J. Physiol. (Lond.)* 453: 219–231, 1992.
32. **Sanger, F., S. Nicklen, and A. K. Carlson.** DNA sequencing with chain-terminating inhibitors. *Proc. Natl. Acad. Sci. USA* 74: 5463–5467, 1977.
33. **Scheuer, T., V. J. Auld, S. Boyd, J. Offord, R. Dunn, and W. A. Catterall.** Functional properties of rat brain sodium channels expressed in a somatic cell line. *Science* 244: 854–858, 1990.
34. **Sigworth, F. J., and S. M. Sine.** Data transformations for improved display and fitting of single-channel dwell time histograms. *Biophys. J.* 52: 1047–1054, 1987.
35. **Smith, P. L., T. Baukrowitz, and G. Yellen.** The inward rectification mechanism of the HERG cardiac potassium channel. *Nature* 379: 833–836, 1996.
36. **Vassilev, P. M., T. Scheuer, and W. A. Catterall.** Identification of an intracellular peptide segment involved in sodium channel inactivation. *Science* 241: 1658–1661, 1988.
37. **Wang, Q., J. Shen, Z. Li, K. Timothy, G. M. Vincent, S. G. Priori, P. J. Schwartz, and M. T. Keating.** Cardiac sodium channel mutations in patients with long QT syndrome, an inherited cardiac arrhythmia. *Hum. Mol. Genet.* 4: 1603–1607, 1995.
38. **Wang, Q., J. Shen, I. Splawski, D. Atkinson, A. Li, J. L. Robinson, A. J. Moss, J. A. Towbin, and M. T. Keating.** SCN5A mutations associated with an inherited cardiac arrhythmia, long QT syndrome. *Cell* 80: 805–811, 1995.
39. **Wasserstrom, J. A., and J. J. Salata.** Basis for tetrodotoxin and lidocaine effects on action potentials in dog ventricular myocytes. *Am. J. Physiol.* 254 (Heart Circ. Physiol. 23): H1157–H1166, 1988.
40. **Wendt, D. J., C. F. Starmer, and A. O. Grant.** Na channel kinetics remain stable during perforated patch recordings. *Am. J. Physiol.* 263 (Cell Physiol. 32): C1234–C1240, 1992.
41. **West, J. W., D. E. Patton, T. Scheuer, Y. Wang, A. L. Goldin, and W. A. Catterall.** A cluster of hydrophobic amino acid residues required for fast Na⁺-channel inactivation. *Proc. Natl. Acad. Sci. USA* 89: 10910–10914, 1992.
42. **Yue, D. T., J. H. Lawrence, and E. Marban.** Two molecular transitions influence cardiac sodium channel gating. *Science* 244: 349–352, 1989.